Improved T-matrix computations for large, nonabsorbing and weakly absorbing nonspherical particles and comparison with geometrical-optics approximation

Dingeman J. Wielaard, Michael I. Mishchenko, Andreas Macke, and Barbara E. Carlson

We show that the use of a matrix inversion scheme based on a special lower triangular–upper triangular factorization rather than on the standard Gaussian elimination significantly improves the numerical stability of **T**-matrix computations for nonabsorbing and weakly absorbing nonspherical particles. As a result, the maximum convergent size parameter for particles with small or zero absorption can increase by a factor of several and can exceed 100. We describe an improved scheme for evaluating Clebsch–Gordon coefficients with large quantum numbers, which allowed us to extend the analytical orientational averaging method developed by Mishchenko [J. Opt. Soc. Am. A **8,** 871 (1991)] to larger size parameters. Comparisons of **T**-matrix and geometrical optics computations for large, randomly oriented spheroids and finite circular cylinders show that the applicability range of the ray-tracing approximation depends on the imaginary part of the refractive index and is different for different elements of the scattering matrix. © 1997 Optical Society of America

Key words: light scattering, nonspherical particles, **T**-matrix method, geometrical optics approximation.

1. Introduction

Waterman's **T**-matrix approach[1] is one of the most powerful exact techniques for computing light scattering by nonspherical particles based on solving Maxwell's equations.[2,3] However, even this method can exhibit convergence problems when any of the variables defining the scattering particle (size parameter, deviation from sphericity, or refractive index) becomes too extreme.[4,5] Standard **T**-matrix computations become especially ill-conditioned for particles with a small or zero imaginary part of the refractive index because of the strong effect of the ripple structure.[6] For example, the maximum convergent equivalent-sphere size parameter (i.e., the ratio of particle circumference to wavelength of scattered light for the surface-equivalent sphere) in double-precision FORTRAN computations for oblate spheroids with a refractive index of 1.53 and an aspect ratio of 2 is only 8, whereas the maximum convergent size parameter for the same particles but with a moderately absorbing refractive index of $1.53 + 0.001i$ is 33. This sensitivity of the standard **T**-matrix procedure to weak or zero absorption has been a serious limiting factor because many commonly encountered substances are weakly absorbing in some spectral ranges. The example of water ice at visible wavelengths[7] is particularly important because quite often a significant fraction of cirrus and contrail ice particles are not much larger than a visible wavelength,[8–11] thus potentially precluding the use of geometrical-optics (GO) approximation in light scattering computations.

In this paper we describe a modified **T**-matrix procedure that has no abnormal sensitivity to weak or zero absorption. This procedure is based on a special matrix inversion scheme and allows efficient computations of nonspherical scattering for particles with size parameters well exceeding 100. To compute light scattering by such large nonspherical particles in random orientation with the analytical

D. J. Wielaard, M. I. Mishchenko, A. Macke, and B. E. Carlson are with the NASA Goddard Institute for Space Studies, 2880 Broadway, New York, New York 10025. D. J. Wielaard and A. Macke are also with the Department of Applied Physics, Columbia University, New York, New York 10025. M. I. Mishchenko is also with the Institute of Terrestrial and Planetary Atmospheres, State University of New York at Stony Brook, Stony Brook, New York 11794.

Received 9 October 1996; revised manuscript received 20 December 1996.

0003-6935/97/184305-09$10.00/0

© 1997 Optical Society of America

method of Ref. 12, we also develop an improved scheme for evaluating Clebsch–Gordan coefficients with large quantum numbers. Finally, we compare exact **T** matrix and approximate GO computations of the Stokes scattering matrix for randomly oriented ice spheroids and finite circular cylinders and further assess the accuracy of GO at lower frequencies.

2. Improved T-Matrix Procedure

The origin of the numerical instability of the standard **T**-matrix procedure for extreme values of particle characteristics is well explained in Refs. 2 and 4. In brief, calculations based on the extended boundary condition method (EBCM)[1] assume the representation of the **T** matrix in the form $\mathbf{T} = -\mathbf{Q}^{-1}\,\mathrm{Rg}\mathbf{Q}$, where the elements of the matrices **Q** and Rg**Q** are integrals over the particle surface. The numerical inversion of the matrix **Q** is usually performed with the standard Gaussian elimination (GE).[5,13,14] Unfortunately, the calculation of the inverse matrix $\mathbf{Q}^{-1}$ is an ill-conditioned procedure[15] strongly affected by round-off errors and by the fact that different elements of the **Q** matrix can differ by many orders of magnitude. As a result, **T**-matrix computations for extreme particle parameters can be poorly convergent and even divergent.

Two methods for overcoming the numerical instability of **T**-matrix computations have been suggested in Refs. 16–18. However, the stability of the method developed in Ref. 16 is achieved at the expense of a considerable increase in computer code complexity and required CPU time, whereas the method developed in Refs. 17 and 18 is applicable only to nonabsorbing particles (i.e., particles with the imaginary part of the refractive index exactly equal to zero or infinity, corresponding to lossless dielectrics and perfect conductors, respectively) and cannot be applied to weakly absorbing scatterers.

Several inversion techniques have been suggested in the literature to deal specifically with ill-conditioned matrices (e.g., Ref. 19). We have tested several such techniques and found that a simple yet universal and highly efficient approach for dealing with the numerical instability of EBCM for nonabsorbing and weakly absorbing particles is to replace the matrix inversion procedure based on GE by a procedure based on a special lower triangular–upper triangular (LU) factorization.[19] The procedure forms the LU factorization of the complex matrix **Q** as $\mathbf{Q} = \mathbf{PLU}$, where **P** is a permutation matrix, **L** is lower triangular with unit diagonal elements, and **U** is upper triangular. The inverse of **Q** is computed by forming $\mathbf{U}^{-1}$ and then solving the equation $\mathbf{XPL} = \mathbf{U}^{-1}$ for **X**. The procedure uses partial pivoting with row interchanges. In our computer code we have adopted the Numerical Algorithms Group FORTRAN Library implementation of this procedure (subroutines F07ARF and F07AWF).[20] Multiple numerical tests performed for particles with different values of the imaginary part of the refractive index have shown that the modified **T**-matrix scheme is much more stable than that based on GE and is not negatively influenced by zero or weak absorption. For a given particle shape and refractive index, the use of the LU-based scheme always increases the maximum convergent equivalent-sphere size parameter $x_{\max}$. The increase is modest (5–20%) for moderately absorbing particles (imaginary part of the refractive index larger than approximately 0.001) but can be as large as a factor of 4 for nonabsorbing and weakly absorbing scatterers. As with the GE-based scheme, the use of extended-precision instead of double-precision floating-point variables[21] further increases the maximum size parameter for which convergence of **T**-matrix computations can be achieved by a factor exceeding 2. Moreover, we have found that in the case of zero absorption, $x_{\max}$ values reached with the universal LU-based **T**-matrix scheme are never smaller than those achieved with the specialized method of Ref. 18, the LU-based scheme being almost twice as fast. In particular, with the LU-based scheme we have been able to reproduce the results given in Tables 1 and 2 of Ref. 18 and successfully treat even larger aspect ratios.

With the improved **T**-matrix scheme, converged **T** matrices can be computed for nonabsorbing and weakly absorbing particles with equivalent-sphere size parameters well exceeding 100. The next computational step is to use the converged **T** matrix in the analytical orientation averaging procedure for calculating the optical cross sections and the Stokes scattering matrix for randomly oriented particles.[12,22] This procedure involves the computation of the so-called Clebsch–Gordon coefficients ${C_{lknm}}^{qp}$ with integer quantum numbers and given l, k, n, and m. By definition,[23] $p \equiv k + m$ and $q_{\min} \le q \le q_{\max}$, where $q_{\min} = \max(|p|, |l - n|)$ and $q_{\max} = l + n$. Furthermore, q is always smaller than or equal to $n_{\max}$, where $n_{\max}$ specifies the size of the converged **T** matrix.[22] Since $n_{\max}$ is always larger than the particle equivalent-sphere size parameter,[5,13,22] for large particles all quantum numbers can well exceed 100. In the exact evaluation of Clebsch–Gordan coefficients with large quantum numbers, one can encounter numerical problems, the origin of which is well documented in Ref. 24. The scheme described in Ref. 12 is based on the computation of Clebsch–Gordan coefficients by use of a three-term upward recursion of the type

$$ {C_{lknm}}^{qp} = A(q){C_{lknm}}^{q-1p} + B(q){C_{lknm}}^{q-2p} \qquad (1) $$

[see Eq. (B2) of Ref. 12] with initial values

$$ {C_{lknm}}^{q_{\min}-1p} = 0, \qquad (2) $$

$$ {C_{lknm}}^{q_{\min}p} = C(q_{\min}), \qquad (3) $$

where $C(q_{\min})$ is given by Eqs. (B3)–(B5) of Ref. 12. We have found, however, that this scheme produces numerically stable results only for $n_{\max}$ values smaller than approximately 60 if double-precision (REAL*8) floating-point FORTRAN variables are used and smaller than approximately 105 if the scheme is implemented in extended-precision (REAL*16) variables.

The instability occurs in those cases when $n_{\max}$ is close or equal to $q_{\max}$ so that the use of the upward recursion of Eq. (1) causes q to reach what Schulten and Gordon[24] call the nonclassical domain of q values. In this domain the absolute value of Clebsch–Gordan coefficients rapidly decays to zero with increasing q. This decay results in a catastrophic loss of numerical accuracy and, ultimately, in overflows.

To stabilize the computation of Clebsch–Gordan coefficients, we have implemented a modified version of the procedure suggested in Ref. 24. Specifically, we use the upward recursion of Eq. (1) only for $q \le q^*$, where $q^* = (q_{\min} + q_{\max})/2$. To compute Clebsch–Gordan coefficients with $q > q^*$, we use the downward recursion analog of Eq. (1),

$$C_{lknm}^{qp} = D(q)C_{lknm}^{q+1p} + E(q)C_{lknm}^{q+2p}, \tag{4}$$

supplemented by two initial values[23]

$$C_{lknm}^{q_{\max}+1p} = 0, \tag{5}$$

$$C_{lknm}^{q_{\max}p} = \times \left[\frac{(2l)!(2n)!(l+n+k+m)!(l+n-k-m)!}{(2l+2n)!(l+k)!(l-k)!(n+m)!(n-m)!}\right]^{1/2}. \tag{6}$$

We have found that because q^* lies in the classical domain in which Clebsch–Gordon coefficients oscillate with a slowly varying amplitude, the two-directional recursion scheme produces highly accurate and numerically stable results for $n_{\max}$ exceeding 150 even when the scheme is implemented in double precision. As a result, the orientation averaging step in actual computer calculations takes only several percent of the time needed to compute the **T** matrix. This fact demonstrates once again the crucial advantage of the analytical orientation averaging method developed in Ref. 12 over the standard procedure based on numerical angle integrations.[5,13,14]

Since the **T**-matrix approach is the only exact technique for the computation of light scattering by randomly oriented nonspherical particles with equivalent-sphere size parameters exceeding 100, the performance of our computer code for the largest convergent size parameters cannot be checked versus independent exact computations. Therefore it was important to make sure that our code does not violate fundamental physical principles and symmetries. Specifically, we have found that our computations of the normalized Stokes scattering matrix

$$F(\Theta) = \begin{bmatrix} F_{11}(\Theta) & F_{12}(\Theta) & 0 & 0 \\ F_{12}(\Theta) & F_{22}(\Theta) & 0 & 0 \\ 0 & 0 & F_{33}(\Theta) & F_{34}(\Theta) \\ 0 & 0 & -F_{34}(\Theta) & F_{44}(\Theta) \end{bmatrix} \tag{7}$$

(as defined in Ref. 12) for randomly oriented rotationally symmetric particles are in full agreement with general equalities[25–28] $F_{12}(0) = F_{12}(\pi) = F_{34}(0) = F_{34}(\pi) = 0$, $F_{22}(0) = F_{33}(0)$, $F_{22}(\pi) = -F_{33}(\pi)$, $F_{11}(\pi) - F_{22}(\pi) = F_{44}(\pi) - F_{33}(\pi)$, and $F_{11}(0) - F_{22}(0) = F_{33}(0) - F_{44}(0)$, as well as with the general inequalities of Refs. 29 and 30. Another important test is to check the conservation of energy, i.e., to verify that the scattering cross section is always smaller than the extinction cross section for absorbing particles and is exactly equal to the extinction cross section for purely nonabsorbing particles. The scattering and extinction cross sections for randomly oriented particles of any shape are given by the following simple analytical formulas[31–33]:

$$C_{\text{sca}} = \frac{2\pi}{k^2}\sum_{n=1}^{n_{\max}}\sum_{n'=1}^{n_{\max}}\sum_{m=-n}^{n}\sum_{m'=-n'}^{n'}\sum_{i=1}^{2}\sum_{j=1}^{2}|T_{\text{mnm'n'}}^{\text{ij}}|^2, \tag{8}$$

$$C_{\text{ext}} = -\frac{2\pi}{k^2}\,\text{Re}\sum_{n=1}^{n_{\max}}\sum_{m=-n}^{n}(T_{mnmn}^{\;\;11} + T_{mnmn}^{\;\;22}), \tag{9}$$

where $T_{mnm'n'}^{\;\;ij}$ are elements of the **T** matrix computed in an arbitrarily chosen reference frame. For rotationally symmetric particles such as spheroids and circular cylinders, the **T** matrix computed in the natural coordinate system with the z axis along the axis of particle symmetry is diagonal with respect to indices m and m',

$$T_{mnm'n'}^{\;\;ij} = \delta_{mm'}T_{mnmn'}^{\;\;ij}, \tag{10}$$

so that Eq. (8) becomes simpler:

$$C_{\text{sca}} = \frac{2\pi}{k^2}\sum_{n=1}^{n_{\max}}\sum_{n'=1}^{n_{\max}}\sum_{m=-\min(n,n')}^{\min(n,n')}\sum_{i=1}^{2}\sum_{j=1}^{2}|T_{mnmn'}^{\;\;ij}|^2. \tag{11}$$

Thus, the energy conservation law requires that

$$\sum_{n=1}^{n_{\max}}\sum_{n'=1}^{n_{\max}}\sum_{m=-\min(n,n')}^{\min(n,n')}\sum_{i=1}^{2}\sum_{j=1}^{2}|T_{mnmn'}^{\;\;ij}|^2 \le -\text{Re}\sum_{n=1}^{n_{\max}}\sum_{m=-n}^{n}(T_{mnmn}^{\;\;11} + T_{mnmn}^{\;\;22}), \tag{12}$$

where the equality holds only for purely nonabsorbing particles. We found that our **T**-matrix computations satisfy the partial inequality (12) with extremely high accuracy.

Inequality (12) involves all the elements of the **T** matrix and is not quite convenient in checking the computer code on a step-by-step basis because, for rotationally symmetric particles, each mth component of the **T** matrix is computed separately.[5,13,22] However, Eq. (12) can be generalized easily so that it includes only the elements of the mth submatrix of the **T** matrix. Specifically, rewriting Eq. (14) on page 180 of Ref. 34 in the form

$$\sum_{ln_1m_1}(T_{m_1n_1mn}^{\;\;\;\;li})^*T_{m_1n_1m'n'}^{\;\;\;\;lj} \le -\frac{1}{2}[(T_{m'n'mn}^{\;\;\;\;ji})^* + T_{mnm'n'}^{\;\;\;\;ij}], \tag{13}$$

where the superscript * denotes a complex conjugate, taking the trace of both sides of Eq. (13) over the indices i, j and n, n', and taking into account Eq. (10),

we derive

$$\sum_{n=1}^{n_{\max}}\sum_{n'=1}^{n_{\max}}\sum_{i=1}^{2}\sum_{j=1}^{2}|T_{mnmn'}{}^{ij}|^2 \le -\mathrm{Re}\sum_{n=1}^{n_{\max}}(T_{mnmn}{}^{11}+T_{mnmn}{}^{22}),$$
$$-\min(n,n') \le m \le \min(n,n'), \quad (14)$$

where the equality holds only for lossless particles. Again, we found that our computer code is perfectly consistent with Eq. (14).

Finally, we have verified that the elements of the **T** matrix generated by our code satisfy the reciprocity relation that, for rotationally symmetric particles, reads[2]

$$T_{mnmn'}{}^{ij} = (-1)^{i+j}T_{mn'mn}{}^{ji}. \quad (15)$$

The high numerical stability and accuracy of our **T**-matrix code make it a reliable source of benchmark results that can be used to check the accuracy of other exact methods for computing nonspherical scattering. Benchmark calculations for nonspherical particles have already been published in several papers (e.g., Refs. 35–38). However, all those calculations pertain to relatively small size parameters and might not be sufficient for testing the most powerful techniques at higher frequencies. Therefore we have used the latest version of the **T**-matrix code to produce benchmark results for a more challenging model consisting of randomly oriented, monodisperse oblate spheroids with an aspect ratio (ratio of the largest to the smallest spheroidal axes) of 2, a surface-equivalent-sphere size parameter of 60, and a refractive index of $1.311 + i0.311 \times 10^{-8}$. The latter corresponds to water ice at a wavelength of 0.55 μm.[7] Table 1 and Fig. 1 show the elements of the Stokes scattering matrix **F** as functions of the scattering angle Θ. At wavelength $\lambda = 2\pi$ μm ≈ 6.283185 μm, the extinction cross section for this model is $C_{\mathrm{ext}} = 24286.0$ μm^2. The single scattering albedo differs from 1 by less than 0.000001, and the asymmetry parameter of the phase function is equal to $\langle\cos\Theta\rangle = 0.813074$. The extinction cross section, the single scattering albedo, the asymmetry parameter, and the table entries are expected to be accurate to within ±1 in the last digits given. The calculation of this benchmark test with a version of the code that used extended-precision floating-point variables took only 50 min of CPU time on an IBM reduced instruction-set computing Model 39H workstation. Note that the pronounced interference structure (see below) necessitated the calculation of the scattering matrix elements in Fig. 1 at 721 equidistant scattering angles 0°(0.25°)180°.

3. Comparisons with Ray Tracing Computations

T-matrix computations for large, randomly oriented spheroids and finite circular cylinders have already been used to check the accuracy of GO at lower frequencies.[39,40] However, the maximum equivalent-sphere size parameter in those calculations was only 60, particles were moderately absorbing, and only the (1,1) and (1,2) elements of the scattering matrix **F** were examined. In this section we extend comparisons of GO and **T**-matrix computations to particles

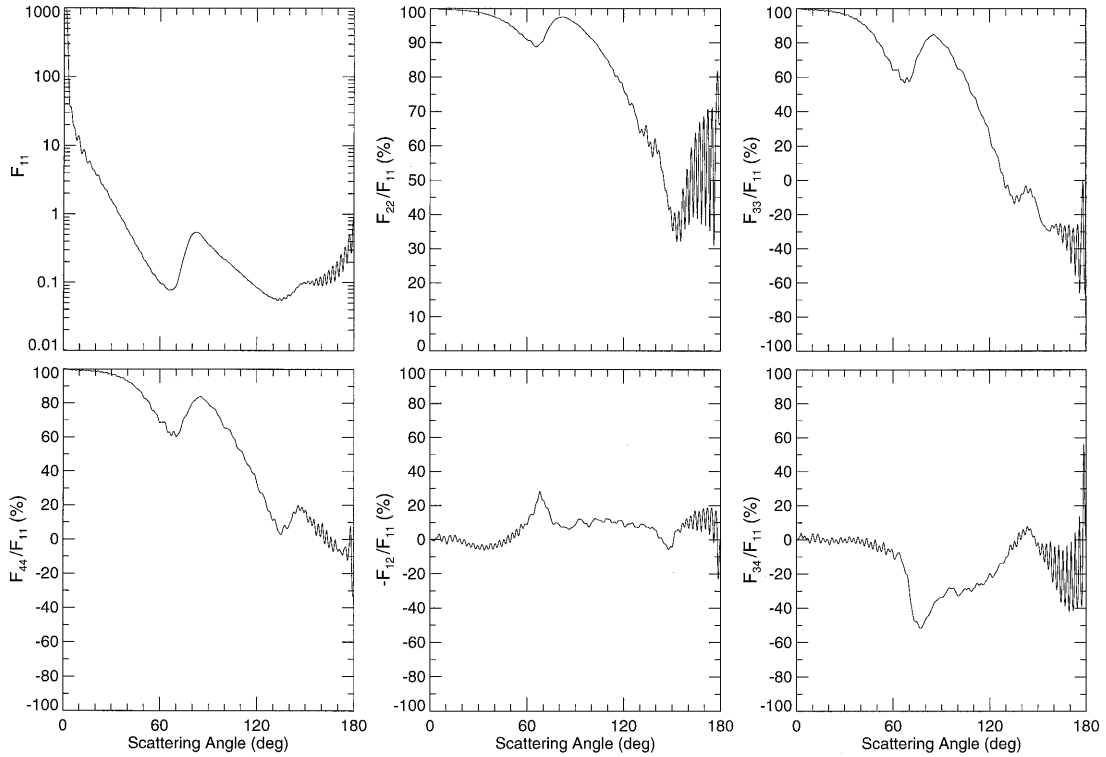

Fig. 1. Scattering matrix elements for randomly oriented, monodisperse oblate spheroids with aspect ratio 2, surface-equivalent-sphere size parameter 60, and refractive index $1.311 + i0.311 \times 10^{-8}$.

Table 1. Scattering Matrix Elements for Randomly Oriented, Monodisperse Oblate Spheroids[a]

Θ (deg)	F_{11}	F_{22}	F_{33}	F_{44}	F_{12}	F_{34}
0	2043.769774	2043.647494	2043.647494	2043.525214	0.000000	0.000000
10	11.103902	11.077070	11.024888	11.017917	0.084554	0.393738
20	3.735759	3.714384	3.675409	3.676258	0.099533	−0.046823
30	1.553804	1.535328	1.501676	1.505878	0.060560	0.004923
40	0.582886	0.568605	0.537073	0.541737	0.017057	−0.011814
50	0.215809	0.204586	0.174740	0.179757	0.002210	−0.012014
60	0.098574	0.089610	0.062918	0.067427	−0.008515	−0.007651
70	0.088448	0.080104	0.050826	0.053448	−0.020528	−0.025399
80	0.505336	0.491971	0.409642	0.405145	−0.044233	−0.235548
90	0.359394	0.344001	0.289166	0.286130	−0.031492	−0.120884
100	0.217290	0.198162	0.141209	0.142219	−0.021323	−0.071015
110	0.137162	0.116535	0.066971	0.071448	−0.016640	−0.039150
120	0.083785	0.063839	0.021942	0.028099	−0.007365	−0.016596
130	0.057918	0.036959	−0.002640	0.006417	−0.004743	−0.006141
140	0.065025	0.039583	−0.005102	0.005515	−0.003684	0.001462
150	0.097288	0.036169	−0.015725	0.016453	0.004170	−0.001993
160	0.102508	0.047010	−0.028308	0.005023	−0.008199	−0.013803
170	0.178125	0.112762	−0.053938	−0.011937	−0.025822	−0.057302
180	0.917684	0.613518	−0.613518	−0.309351	0.000000	0.000000

[a]An aspect ratio of 2, a surface-equivalent-sphere size parameter of 60, and a refractive index of $1.311 + i0.311 \times 10^{-8}$.

with much larger size parameters and essentially zero absorption and to all nonzero elements of the scattering matrix. To this end, we have used the most advanced version of the **T**-matrix code described above and the GO code described in Refs. 41 and 42. Figures 2–5 display **T**-matrix and GO computations of the nonzero scattering matrix elements for the following four models.

Model 1: randomly oriented, monodisperse, nonabsorbing oblate spheroids with an aspect ratio of 2, a surface-equivalent-sphere size parameter of 85, and a refractive index of 1.311.

Model 2: same as Model 1, but with a moderately absorbing refractive index of $1.311 + 0.003i$.

Model 3: randomly oriented, monodisperse, nonabsorbing circular cylinders with a length-to-

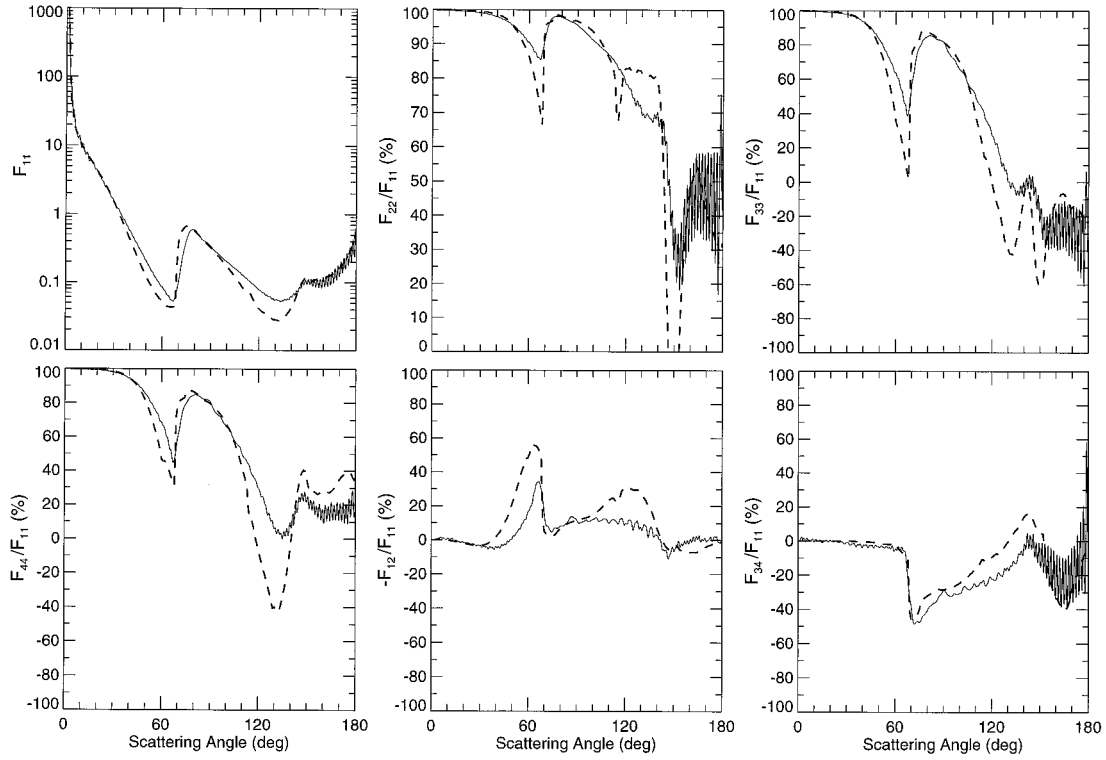

Fig. 2. **T**-matrix (solid curves) and GO (dashed curves) computations of the elements of the scattering matrix for Model 1.

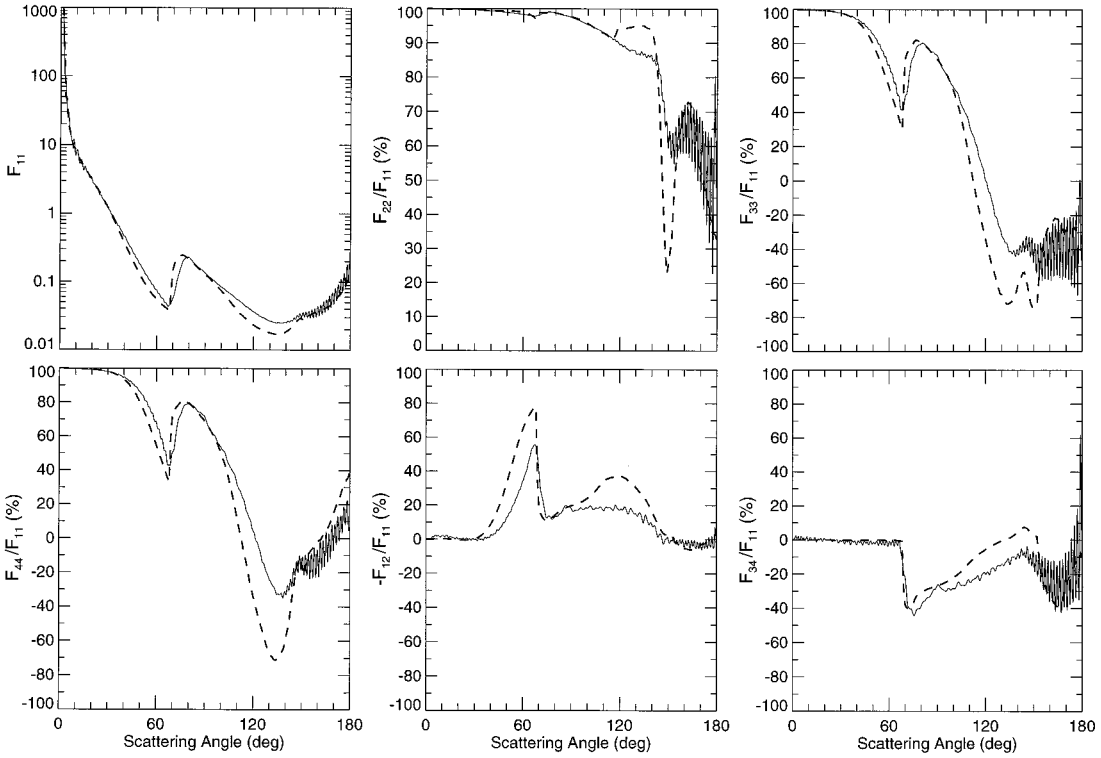

Fig. 3. Same as Fig. 2 but for Model 2.

diameter ratio of 1, a surface-equivalent-sphere size parameter of 125, and a refractive index of 1.311.

Model 4: same as Model 3, but with a moderately absorbing refractive index of $1.311 + 0.003i$.

Figures 2–5 clearly show that the agreement between approximate GO and exact **T**-matrix computations is much better for the phase function, i.e., F_{11}, than for the other elements of the scattering matrix. Furthermore, the agreement is better for moderately absorbing than for nonabsorbing particles. From the phase function standpoint, the spheroids with a size parameter of 85 and the cylinders with a size parameter of 125 are already in the GO domain. Indeed, the **T**-matrix phase function curves show a rainbow-type local maximum at approximately 80° (Figs. 2 and 3) typical of large spheroids and produced by twice refracted and once internally reflected rays,[42,43] and a 46° halo produced by large cylinders (Figs. 4 and 5) caused by minimum deviation at 90° prisms.[42] The strong backscattering peak produced by the cylinders is also a GO feature caused by double internal reflections from mutually perpendicular facets.[38,42] However, GO significantly overestimates the amplitude of the backscattering peak (by a factor of 6.3 for the nonabsorbing cylinders and by a factor of 4.9 for the moderately absorbing cylinders). Because the strong backscattering peak is caused by mutually perpendicular facets, our results indicate a potentially serious problem in applying GO to analyze backscattering measurements (in particular, lidar measurements) of hexagonal ice cloud particles. Note that GO is completely incapable of reproducing the glory for spherical particles,[44] which, along with our results, can suggest that GO computations at the exact backscattering direction can be especially inaccurate. Finally, the GO phase function for the nonabsorbing cylinders (Fig. 4) shows a maximum at 134° (attributed by Yang and Cai[43] to rays incident normally to the cylinder axis) that is not fully reproduced by the exact **T**-matrix computation.

The strong oscillations in the **T**-matrix curves are a manifestation of the interference structure typical of monodisperse particles and caused by interference of light diffracted and reflected or transmitted by a particle.[44] Orientation averaging for nonspherical particles makes the interference structure less pronounced than that for equivalent spheres.[2,45] However, the interference structure in Figs. 2–5 is still strong, especially in the vicinity of the backscattering direction. To resolve the interference structure in Figs. 2–5 fully, we had to perform **T**-matrix computations of the scattering matrix with a scattering angle step size as small as 0.25°. Because GO ignores interference effects, ray-tracing computations cannot reproduce the interference structure exhibited by the exact **T**-matrix curves.

In terms of GO, the angular behavior of linear polarization $-F_{12}/F_{11}$ for particles much larger than a wavelength can be explained by a superposition of positively polarized external reflections with a maximum at the Brewster angle, weakly polarized direct transmissions, and positively polarized internal reflections. The predominantly positive polarization in Figs. 2–5 is caused by the strong contribution from

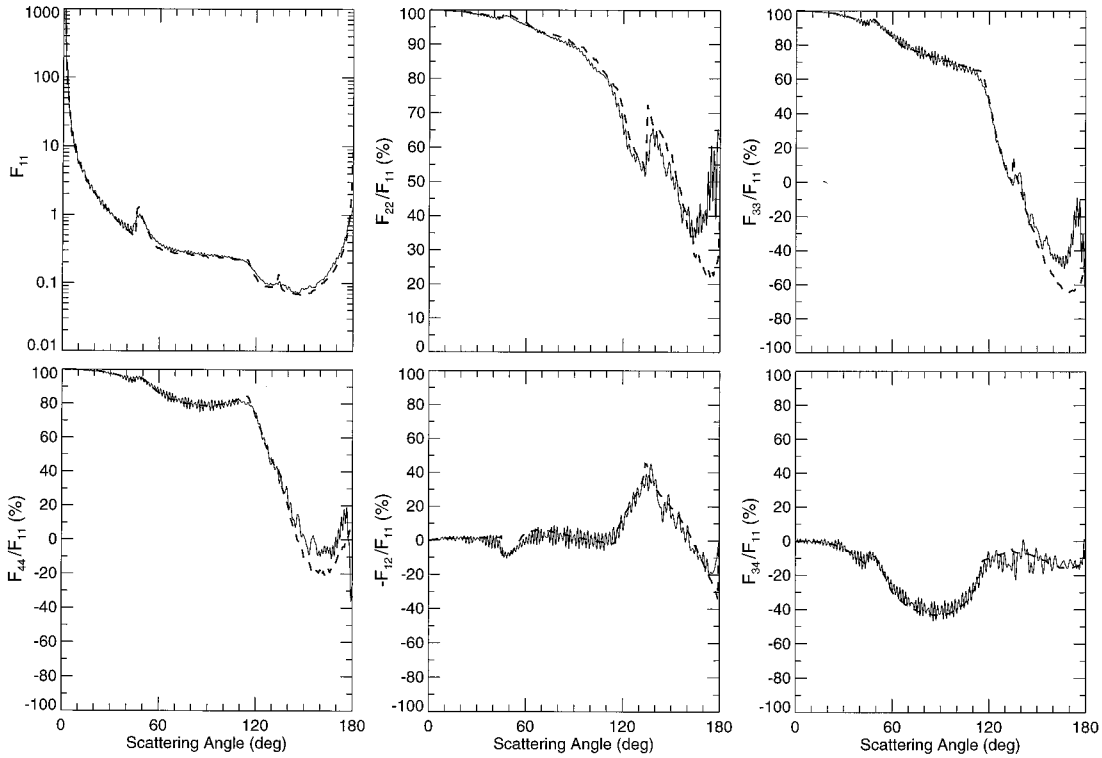

Fig. 4. Same as Fig. 2 but for Model 3.

external reflections. Positively polarized rainbow rays and the deep phase function minimum before the rainbow cause a strong positive polarization maximum at scattering angles just before the rainbow angles for the spheroids. Negatively polarized direct transmissions and tilted facets cause a minimum of negative polarization at the halo angle for the cylinders.

GO and **T**-matrix differences in the scattering matrix elements F_{22}, F_{33}, F_{44}, F_{12}, and F_{34} are almost always much larger than those in the phase function. This means that even such large size parameters as 85 for spheroids and 125 for cylinders are not big enough to make GO calculations of the scattering matrix sufficiently accurate. The differences between the exact and approximate calculations are especially significant for the F_{22} element, thus indicating that the use of GO computations for interpreting lidar depolarization measurements might not be reliable unless particle size parameters exceed a few hundred. In general, GO and **T**-matrix computations for the cylinders are in better agreement than those for the spheroids. This is explained in part by the fact that the cylinder size parameter is almost 1.5 times larger. An additional factor could be the sharp-edged shape of the cylinders, which destroys surface waves and makes the interference effects less pronounced.

4. Concluding Remarks

In this paper we have improved significantly the **T**-matrix technique for computing light scattering by nonspherical particles. Our present **T**-matrix code does not have the abnormal sensitivity to weak or zero absorption typical of the traditional scheme[5,13,14] and can be applied to randomly oriented particles with equivalent-sphere size parameters exceeding 100. The ability of the new **T**-matrix scheme to treat such large size parameters is accompanied by an extremely high numerical efficiency, which makes our code orders of magnitude faster than any alternative technique for exactly computing light scattering by nonspherical particles in random orientation. The unique capabilities of the **T**-matrix code make it very useful in practice but also make checks of its numerical accuracy difficult because independent results for the largest size parameters cannot be obtained with any other currently available method. Therefore we have made sure that our calculations fully satisfy such fundamental physical constraints as symmetry, reciprocity, and energy conservation. Also, we have presented benchmark results for a challenging test case that can be used for checking the accuracy of the most advanced nonspherical scattering codes at higher frequencies.

By use of the present version of the **T**-matrix code, we have continued the work initiated in Refs. 39 and 40 and extended comparisons of exact **T**-matrix and approximate ray-tracing calculations to much larger size parameters and to all elements of the scattering matrix. Our results suggest that equivalent-sphere size parameters larger than approximately 80 are already big enough to ensure acceptable accuracy of GO phase function computations (except, perhaps, at exactly the backscattering direction). However, GO calculations of the other elements of the scattering

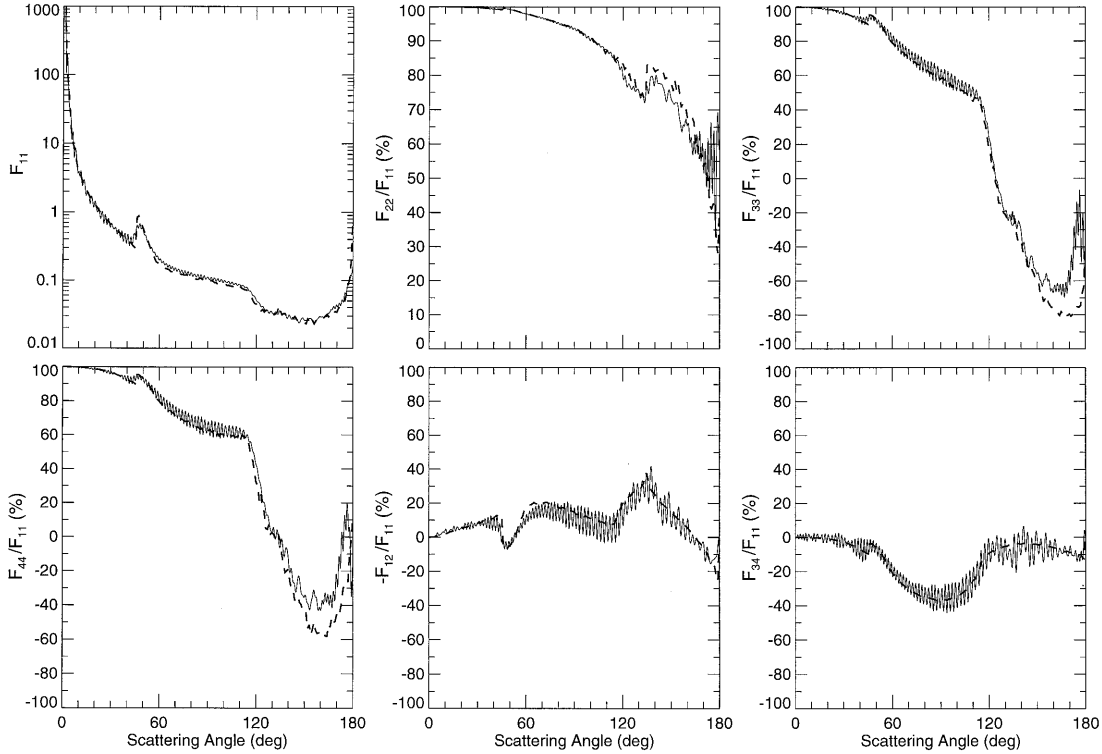

Fig. 5. Same as Fig. 2 but for Model 4.

matrix are strongly affected by wave effects and become reasonably accurate only at significantly larger size parameters. GO calculations of lidar depolarization can be expected to be especially inaccurate unless the equivalent-sphere size parameter exceeds several hundred.

An interesting result of our calculations is that the **T**-matrix method can be applied successfully to large, sharp-edged particles such as finite circular cylinders with equivalent-sphere size parameters exceeding 100. It has been claimed often that the presence of sharp edges can be difficult to handle with a method that uses smooth spherical functions in the internal and scattered field decompositions. We have found, however, that the use of a special numerical integration scheme for computing the surface integrals needed to calculate the **T** matrix[38] ameliorates the problem of sharp edges and makes **T**-matrix computations for cylinders almost as accurate as those for surface- and aspect-ratio-equivalent smooth-shaped spheroids. Much more difficult problems are encountered when the **T**-matrix method is applied to particles with large aspect ratios. In this case a single spherical function expansion of the internal and scattered fields can fail, and the use of several overlapping subdomain spherical function expansions may become necessary, as suggested in Ref. 16. A similar approach based on approximation of the surface field by use of lowest-order multipoles located in the complex plane has been developed in Ref. 46.

We are grateful to L. D. Travis for many useful discussions, to J. L. Haferman for a constructive review, to E. Ravin for programming support, and to N. T. Zakharova for programming support and help with graphics. This research was funded by a NASA First International Satellite Cloud Climatology Project Regional Experiment (FIRE) III grant.

The **T**-matrix code described in this paper is available at the web site http://www.giss.nasa.gov/~crmim.
Address all correspondence to M. I. Mishchenko: telephone, 212-678-5528; fax, 212-678-5552; e-mail, crmim@giss.nasa.gov.

References

1. P. C. Waterman, "Symmetry, unitarity, and geometry in electromagnetic scattering," Phys. Rev. D **3,** 825–839 (1971).
2. M. I. Mishchenko, L. D. Travis, and D. W. Mackowski, "**T**-matrix computations of light scattering by nonspherical particles: a review," J. Quantum Spectrosc. Radiat. Transfer **55,** 535–575 (1996).
3. M. I. Mishchenko, L. D. Travis, and A. Macke, "Light scattering by nonspherical particles in the atmosphere: an overview," in *International Radiation Symposium '96: Current Problems in Atmospheric Radiation*, W. L. Smith and K. Stamnes, eds. (Deepak, Hampton, Va., 1996).
4. P. W. Barber, "Resonance electromagnetic absorption by nonspherical dielectric objects," IEEE Trans. Microwave Theory Tech. **MTT-25,** 373–381 (1977).
5. W. J. Wiscombe and A. Mugnai, "Single scattering from nonspherical Chebyshev particles: a compendium of calculations," NASA Ref. Publ. 1157 (NASA Goddard Space Flight Center, Greenbelt, Md., 1986).

6. A. Mugnai and W. J. Wiscombe, "Scattering from nonspherical Chebyshev particles. 1: Cross sections, single-scattering albedo, asymmetry factor, and backscattered fraction," Appl. Opt. **25,** 1235–1244 (1986).
7. S. G. Warren, "Optical constants of ice from the ultraviolet to the microwave," Appl. Opt. **23,** 1206–1225 (1984).
8. C. M. R. Platt, J. D. Spinhirne, and W. D. Hart, "Optical and microphysical properties of a cold cirrus cloud: evidence for regions of small ice particles," J. Geophys. Res. **94,** 11,151–11,164 (1989).
9. C. Prabhakara, J.-M. Yoo, G. Dalu, and R. S. Fraser, "Deep optically thin cirrus clouds in the polar regions. Part I: Infrared extinction characteristics," J. Appl. Meteorol. **29,** 1313–1329 (1990).
10. S. Kinne, T. P. Ackerman, A. J. Heymsfield, F. P. J. Valero, K. Sassen, and J. D. Spinhirne, "Cirrus microphysics and radiative transfer: cloud field study on 28 October 1986," Mon. Weather Rev. **120,** 661–684 (1992).
11. W. P. Arnott, Y. Y. Dong, J. Hallett, and M. R. Poelott, "Role of small ice crystals in radiative properties of cirrus: a case study, FIRE II, November 22, 1991," J. Geophys. Res. **99,** 1371–1381 (1994).
12. M. I. Mishchenko, "Light scattering by randomly oriented axially symmetric particles," J. Opt. Soc. Am. A **8,** 871–882 (1991); **9,** 497(E) (1992).
13. P. W. Barber and S. C. Hill, *Light Scattering by Particles: Computational Methods* (World Scientific, Singapore, 1990).
14. F. Y. Sid'ko, V. N. Lopatin, and L. E. Paramonov, *Polarization Characteristics of Suspensions of Biological Particles* (Nauka, Novosibirsk, 1990), in Russian.
15. W. H. Press, S. A. Teukolsky, W. T. Vetterling, and B. P. Flannery, *Numerical Recipes in FORTRAN: The Art of Scientific Computing* (Cambridge U. Press, Cambridge, U.K., 1992).
16. M. F. Iskander and A. Lakhtakia, "Extension of the iterative EBCM to calculate scattering by low-loss or lossless elongated dielectric objects," Appl. Opt. **23,** 948–953 (1984).
17. P. C. Waterman, "Numerical solution of electromagnetic scattering problems," in *Computer Techniques for Electromagnetics*, R. Mittra, ed. (Pergamon, Oxford, 1973), pp. 97–157.
18. A. Lakhtakia, V. K. Varadan, and V. V. Varadan, "Scattering by highly aspherical targets: EBCM coupled with reinforced orthogonalization," Appl. Opt. **23,** 3502–3504 (1994).
19. G. H. Golub and C. F. van Loan, *Matrix Computations*, (Johns Hopkins U. Press, Baltimore, Md., 1989), Chap. 3.
20. *NAG FORTRAN Library Manual, Mark 15* (Numerical Algorithms Groups, Oxford, U. K., 1991).
21. M. I. Mishchenko and L. D. Travis, "**T**-matrix computations of light scattering by large spheroidal particles," Opt. Commun. **109,** 16–21 (1994).
22. M. I. Mishchenko, "Light scattering by size-shape distributions of randomly oriented axially symmetric particles of a size comparable to a wavelength," Appl. Opt. **32,** 4652–4666 (1993).
23. D. A. Varshalovich, A. N. Moskalev, and V. K. Khersonskii, *Quantum Theory of Angular Momentum: Irreducible Tensors, Spherical Harmonics, Vector Coupling Coefficients, 3nj Symbols* (World Scientific, Singapore, 1988).
24. K. Schulten and R. G. Gordon, "Exact recursive evaluation of 3*j*- and 6*j*-coefficients for quantum-mechanical coupling of angular momenta," J. Math. Phys. **16,** 1961–1970 (1975).
25. H. C. van de Hulst, *Light Scattering by Small Particles* (Wiley, New York, 1957).
26. C. R. Hu, G. W. Kattawar, M. E. Parkin, and P. Herb, "Symmetry theorems on the forward and backward scattering Mueller matrices for light scattering from a nonspherical dielectric scatterer," Appl. Opt. **26,** 4159–4173 (1987).
27. M. I. Mishchenko and L. D. Travis, "Light scattering by polydispersions of randomly oriented spheroids with sizes comparable to wavelengths of observation," Appl. Opt. **33,** 7206–7225 (1994).
28. M. I. Mishchenko and J. W. Hovenier, "Depolarization of light backscattered by randomly oriented nonspherical particles," Opt. Lett. **20,** 1356–1358 (1995).
29. J. W. Hovenier, H. C. van de Hulst, and C. V. M. van der Mee, "Conditions for the elements of the scattering matrix," Astron. Astrophys. **157,** 301–310 (1986).
30. C. V. M. van der Mee and J. W. Hovenier, "Expansion coefficients in polarized light transfer," Astron. Astrophys. **228,** 559–568 (1990).
31. M. I. Mishchenko, "Extinction of light by randomly-oriented non-spherical grains," Astrophys. Space Sci. **164,** 1–13 (1990).
32. M. I. Mishchenko, "Scattering cross section for randomly oriented particles of arbitrary shape," Kinem. Phys. Celest. Bodies **7**(5), 93–95 (1991).
33. N. G. Khlebtsov, "Orientational averaging of light-scattering observables in the **T**-matrix approach," Appl. Opt. **31,** 5359–5365 (1992).
34. L. Tsang, J. A. Kong, and R. T. Shin, *Theory of Microwave Remote Sensing* (Wiley, New York, 1985).
35. F. Kuik, J. F. de Haan, and J. W. Hovenier, "Benchmark results for single scattering by spheroids," J. Quant. Spectrosc. Radiat. Transfer **47,** 477–489 (1992).
36. M. I. Mishchenko and D. W. Mackowski, "Electromagnetic scattering by randomly oriented bispheres: comparison of theory and experiment and benchmark calculations," J. Quant. Spectrosc. Radiat. Transfer **55,** 683–694 (1996).
37. J. W. Hovenier, K. Lumme, M. I. Mishchenko, N. V. Voshchinnikov, D. W. Mackowski, and J. Rahola, "Computations of scattering matrices of four types of non-spherical particles using diverse methods," J. Quant. Spectrosc. Radiat. Transfer **55,** 695–705 (1996).
38. M. I. Mishchenko, L. D. Travis, and A. Macke, "Scattering of light by polydisperse, randomly oriented, finite circular cylinders," Appl. Opt. **35,** 4927–4940 (1996).
39. A. Macke, M. I. Mishchenko, K. Muinonen, and B. E. Carlson, "Scattering of light by large nonspherical particles: ray tracing approximation versus **T**-matrix method," Opt. Lett. **20,** 1934–1936 (1995).
40. A. Macke, M. I. Mishchenko, B. E. Carlson, and K. Muinonen, "Scattering of light by large spherical, spheroidal, and circular cylindrical scatterers: geometrical optics approximation versus **T**-matrix method," in *IRS '96: Current Problems in Atmospheric Radiation*, W. L. Smith and K. Stamnes, eds. (Deepak, Hampton, Va., 1996).
41. A. Macke, J. Mueller, and E. Raschke, "Single scattering properties of atmospheric ice crystals," J. Atmos. Sci. **53,** 2813–2825 (1996).
42. A. Macke and M. I. Mishchenko, "Applicability of regular particle shapes in light scattering calculations for atmospheric ice particles," Appl. Opt. **35,** 4291–4296 (1996).
43. P. Yang and Q. Cai, "Light scattering phase matrices for spheroidal and cylindric large particles," Chinese J. Atmos. Sci. **14,** 345–358 (1991).
44. J. E. Hansen and L. D. Travis, "Light scattering in planetary atmospheres," Space Sci. Rev. **16,** 527–610 (1974).
45. M. I. Mishchenko and L. D. Travis, "Light scattering by polydisperse, rotationally symmetric nonspherical particles: linear polarization," J. Quant. Spectrosc. Radiat. Transfer **51,** 759–778 (1994).
46. A. Doicu and T. Wriedt, "Extended boundary condition method with multipole sources localized in the complex plane," Opt. Commun. (1997).